

# Cannabinoid receptor 1 is a potential drug target for treatment of translocation-positive rhabdomyosarcoma

Susanne Oesch,<sup>1</sup> Dagmar Walter,<sup>1</sup> Marco Wachtel,<sup>1</sup> Kathya Pretre,<sup>1</sup> Maria Salazar,<sup>2</sup> Manuel Guzmán,<sup>2</sup> Guillermo Velasco,<sup>2</sup> and Beat W. Schäfer<sup>1</sup>

<sup>1</sup>Department of Oncology, University Children's Hospital, Zurich, Switzerland and <sup>2</sup>Department of Biochemistry and Molecular Biology 1, School of Biology, Complutense University, Madrid, Spain

## Abstract

Gene expression profiling has revealed that the gene coding for cannabinoid receptor 1 (CB1) is highly up-regulated in rhabdomyosarcoma biopsies bearing the typical chromosomal translocations PAX3/FKHR or PAX7/FKHR. Because cannabinoid receptor agonists are capable of reducing proliferation and inducing apoptosis in diverse cancer cells such as glioma, breast cancer, and melanoma, we evaluated whether CB1 is a potential drug target in rhabdomyosarcoma. Our study shows that treatment with the cannabinoid receptor agonists HU210 and  $\Delta^9$ -tetrahydrocannabinol lowers the viability of translocation-positive rhabdomyosarcoma cells through the induction of apoptosis. This effect relies on inhibition of AKT signaling and induction of the stress-associated transcription factor p8 because small interfering RNA-mediated down-regulation of p8 rescued cell viability upon cannabinoid treatment. Finally, treatment of xenografts with HU210 led to a significant suppression of tumor growth *in vivo*. These results support the notion that cannabinoid receptor agonists could represent a novel targeted approach for treatment of translocation-positive rhabdomyosarcoma. [Mol Cancer Ther 2009;8(7):1838–45]

## Introduction

Rhabdomyosarcoma (RMS) is the most common soft-tissue sarcoma in children, representing 5% to 8% of all childhood malignancies (1). It is believed to originate from muscle precursor cells and histology recognizes two major subtypes: The embryonal subtype (eRMS) accounts for ~60% of

RMS cases and has a rather good prognosis (2). The alveolar subtype (2) is less frequent, more aggressive, usually presents with metastasis, and is thus associated with rather poor treatment outcome. Although no consistent genetic alterations have been identified thus far in eRMS, ~80% of aRMS patients display typical chromosomal translocations t(2;13)(q35;q14) or t(1;13)(p36;q14) encoding for fusion proteins PAX3/FKHR or PAX7/FKHR, respectively (3). These chimeric transcription factors are oncogenic and presumably act mainly through their gain in transcriptional activity. To provide insight into molecular changes elicited by these transcription factors and to find new potential therapeutic targets for treatment of aRMS, gene expression analysis was done in a range of RMS biopsies by several research groups (4–6). These studies consistently revealed a gene expression signature of up-regulated genes in translocation-positive versus translocation-negative samples. Interestingly, translocation-negative aRMS clustered together with eRMS samples in these analyses. Hence, at the molecular level, RMS can be divided into translocation-positive RMS (tposRMS) and translocation-negative RMS (tnegRMS).

The gene expression signature of tposRMS contains a number of receptor molecules that might be potentially amenable as drug targets. Among these, receptors such as c-met have already been validated as therapeutic target (7). However, one of the top-ranking genes in this signature is the cannabinoid receptor 1 (CB1). Thus far, no studies have been undertaken to assess whether CB1 might serve as a future target for therapeutic intervention in this tumor. Evidence exists since 1975 that cancer cell growth can be inhibited by treatment with cannabinoid receptor agonists, as first described by Munson et al. in Lewis lung carcinoma cells (8). Since then, additional cancer cell types such as glioblastoma (9), breast carcinoma (10), or melanoma (11) were reported to be sensitive to the antiproliferative action of cannabinoids. In general, the antitumoral actions of diverse cannabinoid receptor agonists are mediated through the cannabinoid receptor types CB1 and CB2, as reviewed by Guzman et al. (12). Notably, not only *in vitro* cell culture systems are subject to this treatment response but also *in vivo* experiments using either xenografts or syngeneic mouse models have shown the potential of cannabinoids as anti-cancer agents, without observing major psychoactive or immune-suppressive effects (8, 13). Recently, the first clinical study using  $\Delta^9$ -tetrahydrocannabinol (THC) in severe cases of glioblastoma has been reported (14).

At the molecular level, cannabinoids trigger changes in various signaling pathways in cancer cells. One of the primary events after cannabinoid treatment is a sustained *de novo* synthesis of the lipid second messenger ceramide, which in turn is followed by inhibition of AKT signaling (15). Strikingly, both of these signaling events mark a

Received 12/17/08; revised 3/20/09; accepted 4/3/09; published OnlineFirst 6/9/09.

**Grant support:** OncoSuisse grants 01473-02-2004 and 01944.08-2006.

The costs of publication of this article were defrayed in part by the payment of page charges. This article must therefore be hereby marked *advertisement* in accordance with 18 U.S.C. Section 1734 solely to indicate this fact.

**Requests for reprints:** Beat W. Schäfer, Department of Oncology, University Children's Hospital, Steinwiesstrasse 75, 8032 Zurich, Switzerland. Phone: 41-44-266-75-53; Fax: 41-44-266-71-71. E-mail: beat.schaefer@kispi.uzh.ch

Copyright © 2009 American Association for Cancer Research.

doi:10.1158/1535-7163.MCT-08-1147

major difference between tumor cells and healthy non-transformed cells, which undergo AKT activation without *de novo* synthesis of ceramide after cannabinoid stimulation (16). In parallel to AKT inhibition, alterations in extracellular signal-regulated kinase (ERK) signaling have been reported. However, depending on tumor type, either inhibition (17) or sustained activation (18) has been observed. Recently, the stress-associated transcription factor p8 was found to be critically involved in cannabinoid-induced apoptosis of cancer cells (19) as its down-regulation could rescue viability of various cancer cells (20, 21). At the end of the signaling cascade, tumor cells either undergo cell cycle arrest (22, 23) or apoptosis (9, 24).

To improve the treatment outcome of the aggressive tposRMS subtype, novel targeted therapies are urgently needed. Therefore, this study aimed to characterize the effects of cannabinoids on tposRMS cells *in vitro* as well as *in vivo*. Our results show that the CB1 receptor could represent a potential molecular target for future therapeutic approaches in tposRMS.

## Materials and Methods

### Cannabinoids

HU210 [(–)-1,1-dimethylheptyl analogue of 11-hydroxy- $\Delta^8$ -tetrahydrocannabinol] was purchased from Tocris, 2-methyl-2'-F-anandamide (Met-F-AEA) from Cayman, AM251 (analogue of SR141716A) from Sigma-Aldrich, and THC from The Health Concept. All substances were solved in DMSO. For *in vitro* experiments, they were applied at final DMSO concentrations of maximally 0.05% (v/v). For *in vivo* experiments, HU210 was prepared at 0.25% DMSO (v/v) and diluted in PBS supplemented with 5 mg/mL bovine serum albumin.

### Cell Culture

Rh4 and Rh28 tposRMS cells were kindly provided by P. Houghton (St Jude Children's Research Hospital, Memphis, TN, USA). RMS13, RD, and MRC-5 lung fibroblast cells were obtained from the American Type Culture Collection (LGC Promochem). All cells were routinely maintained in DMEM supplemented with 10% FCS. When performing viability or signaling experiments, cells were plated at a density of 17,000/cm<sup>2</sup>, allowed to adhere overnight, and transferred to serum-free medium 6 h before starting drug treatments.

### Cell Viability and Apoptosis Detection

Cell viability was evaluated in 96-well plates using methylthiazolyldiphenyl-tetrazolium bromide from Sigma-Aldrich. Apoptosis was either analyzed with CaspGLOW red active caspase-3 staining kit (Biovision), allowing labeling of apoptotic cells with a fluorescent caspase-3 substrate and subsequent detection by fluorescence microscopy. Alternatively, the apoptosis-indicating ratio of cleaved to uncleaved poly(ADP-ribose)polymerase (PARP) protein was determined densitometrically by Western blotting.

### Reverse Transcriptase-PCR

RNA was extracted with the RNeasy Mini Kit (Qiagen), including a DNase digestion step with RNase-free DNase (Qiagen). One microgram of total RNA was reverse transcribed

with random hexamer primers using the High Capacity cDNA Reverse Transcriptase Kit (Applied Biosystems). PCR was done with primers for hCB1 (5'-CGTGGGCAGCCTGTTCCCTCA-3' and 5'-CATGCGGGCTTGGTCTGG-3') and for glyceraldehyde-3-phosphate dehydrogenase (GAPDH; Microsynth) using the following parameters: After initial denaturation at 94°C for 5 min, cycles (40 $\times$ ) with 94°C for 30 s, 55°C for 30 s, and 72°C for 45 s was done, followed by a final extension at 72°C for 5 min.

### Quantitative Real-time PCR

Quantitative reverse transcription-PCR (RT-PCR) was done under universal cycling parameters on an ABI7900HT instrument using commercially available Mastermix and target probes for CB1, p8, and GAPDH (all from Applied Biosystems). Cycle threshold (C<sub>T</sub>) values were normalized to GAPDH. Relative expression levels of the target genes among the different samples were calculated using the  $\Delta\Delta C_T$  method.

### Gene Silencing

Rh4 cells were transfected with 10 nmol/L small interfering RNA (siRNA) against human p8 (Qiagen) or scrambled siRNA (Ambion) using GeneEraser (Stratagene). One day after siRNA transfection, equal numbers of cells were plated for subsequent viability experiments. p8 down-regulation efficiency was verified by means of quantitative RT-PCR.

### Western Blot Analysis

For detection of intracellular signaling proteins, whole-cell extract was produced with a lysis buffer consisting of 50 mmol/L Tris (pH 7.5), 1% Triton X-100, 1 mmol/L EGTA, 50 mmol/L NaF, 10 mmol/L sodium  $\beta$ -glycerophosphate, 5 mmol/L sodium PPI, 1 mmol/L sodium orthovanadate, 1% phenylmethylsulfonyl fluoride, 0.1%  $\beta$ -mercaptoethanol, and protease inhibitor cocktail complete (Roche) according to standard protocols. Samples were sonicated and equal amounts of protein were used for Western blotting with the NuPAGE system (Invitrogen). Antibodies used for detection included rabbit antibodies raised against CB1 (1:1,000; Affinity Bioreagents), PARP, phospho-AKT (Ser<sup>473</sup>), phospho-AKT (Thr<sup>308</sup>), AKT-total, phospho-ERK (Thr<sup>202</sup>/Tyr<sup>204</sup>), ERK-total, phospho-GSK (Ser<sup>21/9</sup>), and GSK (all 1:1,000; from Cell Signaling Technology). Detection of actin with a rabbit antibody (1:2,000; Sigma-Aldrich) was used to control for equal protein loading. As secondary antibody, an anti-rabbit antibody conjugated to horseradish peroxidase (1:2,000; Pierce) was used. Detection was done with ECL technology (Amersham).

### Confocal Microscopy

Cells on coverslips were fixed with paraformaldehyde (PFA) and incubated with anti-CB1 antibody (1:500; Affinity Bioreagents) in PBS/2.5% goat serum for 0.5 hours at 37°C. For visualization, a secondary anti-rabbit antibody labeled with Alexa Fluor 594 (1:500; Molecular Probes) was used. Control immunostainings using the secondary antibody alone were done in parallel. Confocal fluorescence images were acquired using Laser Sharp 2000 software (Bio-Rad) and a Confocal Radiance 2000 coupled to an Axiovert S100 TV microscope (Carl Zeiss).

### Immunohistochemical Staining

Tumors were fixed, embedded in paraffin, and sectioned into 2- $\mu$ m slices. Immunohistochemical stainings for Ki67 (Lab Vision Corporation) and cleaved caspase-3 (Cell Signaling Technology) were done on the Ventana Benchmark automated staining system (Ventana Medical Systems).

### Tumorigenicity Assay

Rh4 cells ( $7.5 \times 10^6$ ) in 100  $\mu$ L PBS were injected s.c. into the flank of NOD/LtSz-scid IL2R $\gamma$  null (NOG) mice (The Jackson Laboratory). When tumors reached a size of 150 mm<sup>3</sup>, mice were randomly assigned to treatment and control groups and injected peritumorally for 13 d with 0.2 mg/kg HU210 or vehicle (DMSO) alone. Tumor growth was monitored daily with external caliper, and the tumor volume was calculated as  $(4\pi/3)((\text{width} + \text{length})/4)^3$ . Animals were sacrificed 1 d after the last treatment.

### Statistical Analysis

Statistical analysis was done with two-tailed *t* test with the statistics program SPSS. For analysis of tumor growth, a longitudinal analysis was done by comparing linear regressions of the two groups.

## Results

### The CB1 Receptor Is Up-Regulated in Translocation-Positive RMS

Gene expression profiling of RMS biopsy samples shows a signature for tposRMS (4) that includes, as one of the top-ranking genes, *CNR1*, encoding the CB1 receptor (Fig. 1A). In contrast, transcript levels of the related *CNR2* gene, encoding the CB2 receptor, were only slightly above background. To validate the up-regulation of CB1 in tposRMS cells on both the RNA and protein levels, we first applied conventional RT-PCR, which revealed a higher expression of CB1 mRNA in all tposRMS cells than in control cell lines MRC-5 (fibroblast) and RD (eRMS; Fig. 1B). Indeed, expression was >10,000-fold higher than in the controls when assessed quantitatively. In addition, expression of CB1 is 430-fold higher than expression of CB2 in Rh4 cells, whereas in U87MG glioma and A375 melanoma cells, expression of CB2 is more prevalent (data not shown). Further, CB1 was expressed in Rh4 cells also at the protein level as shown by Western blot (Fig. 1C). Last, confocal microscopy of cultured Rh4 and RD cells (Fig. 1D) showed higher immunofluorescence staining intensities for CB1 in Rh4 cells. Hence, expression of CB1 is evident both on the mRNA and protein levels in tposRMS cells, confirming the previous findings using gene expression profiling.

### Cannabinoids Reduce the Viability of tposRMS Cells *In vitro*

After validating the expression of CB1 in tposRMS cells, we next assessed the cell viability after treatment with different cannabinoid receptor agonists. Treatment with the mixed cannabinoid receptor agonist HU-210 reduced the viability of two tposRMS cell lines in a dose-dependent manner (Fig. 2A). Similarly, the main active component of marijuana (THC) as well as the anandamide-related compound Met-F-AEA reduced the viability of Rh4 cells in a

dose-dependent manner but not of the tnegRMS cells (RD) or control nontransformed fibroblasts (MRC-5), which express lower levels of the CB1 receptor (Fig. 2C and D). Finally, pharmacologic blockade of the CB1 receptor significantly restored cell viability of Rh4 cells from 29.2% ( $\pm 2.4$ SD) to 71.9% ( $\pm 11.2$  SD; Fig. 2B), supporting the notion that the observed reduction in cell viability was specifically mediated through the CB1 receptor.

### Cannabinoids Induce Apoptosis in tposRMS Cells

To determine whether decreased cell viability in tposRMS cells after cannabinoid treatment is due to apoptosis, caspase-3 activation and PARP cleavage were analyzed. First, tposRMS cells were treated with 1.25  $\mu$ mol/L HU210 and cell extracts

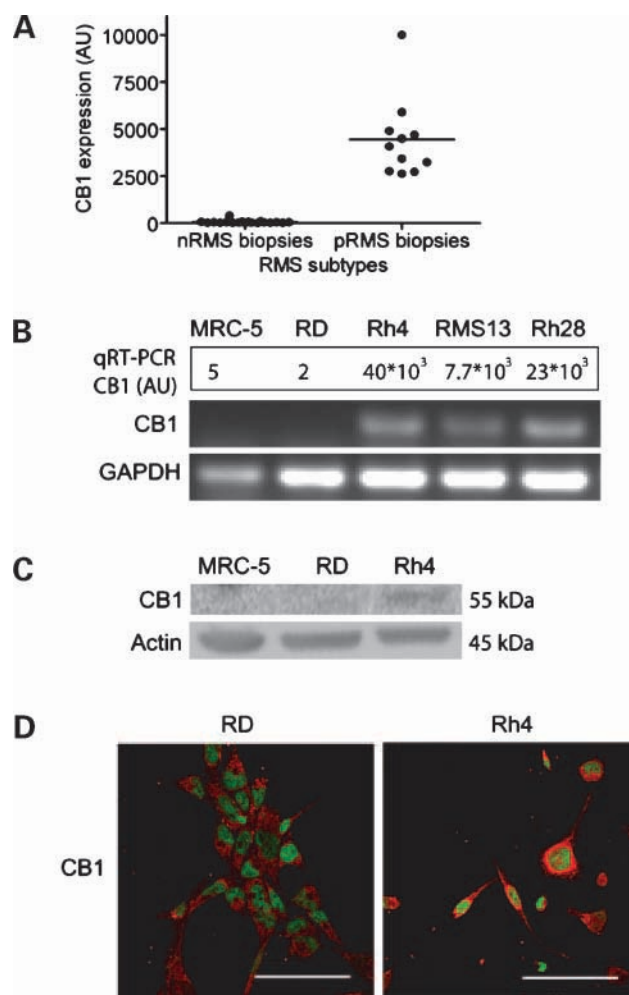
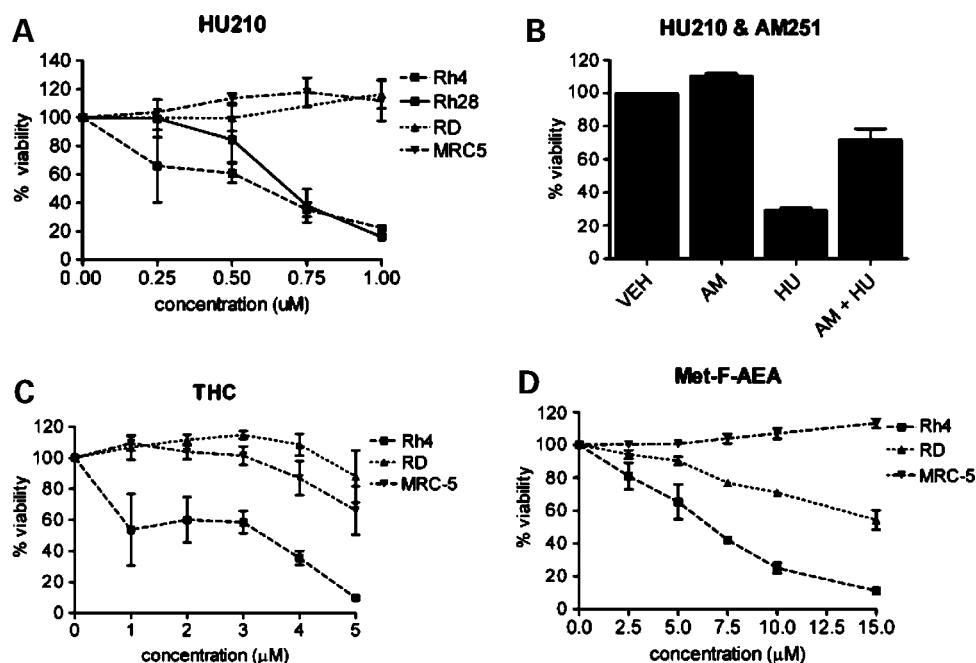


**Figure 1.** CB1 expression in tposRMS cells. **A**, gene expression values of CB1 are shown in arbitrary units. Samples analyzed by microarray gene expression profiling were translocation-negative (tnegRMS) versus translocation-positive (tposRMS) biopsy samples. **B**, quantitative and normal RT-PCR with primers for CB1 and for GAPDH were done with cDNA of cell lines MRC-5 (fibroblast); RD (tnegRMS); and Rh4, Rh28, and RMS13 (all tposRMS) cells. Quantitative results are indicated in arbitrary units. **C**, CB1 protein levels of MRC-5, RD, and Rh4 cells were determined by Western blotting. **D**, confocal images of immunofluorescence stainings with anti-CB1 antibody (red fluorescence) on RD and Rh4 cells (scale bar, 100  $\mu$ m).

**Figure 2.** Cannabinoids reduce viability of tposRMS cells. **A**, cell lines Rh4, Rh28 (tpoS RMS), RD (tnegRMS), and MRC-5 (fibroblasts) were incubated with increasing concentrations of HU210 for 72 h. Subsequent viability measurements by means of MTT are shown ( $n = 3$ ,  $\pm$ SE; significance at  $1.25 \mu\text{mol/L}$ :  $P < 0.005$ ). **B**, viability measurements are shown for Rh4 cells preincubated with vehicle or with  $0.5 \mu\text{mol/L}$  AM251 before undergoing subsequent treatment with  $1 \mu\text{mol/L}$  HU210 for 24 h ( $n = 3$ ,  $\pm$ SE, significance:  $P < 0.05$ ). **C** and **D**, dose-dependent viability of Rh4, RD, and MRC-5 cells after treatment with THC for 24 h or Met-F-AEA for 48 h was measured ( $n = 3$ ,  $\pm$ SE, significance at  $5 \mu\text{mol/L}$  THC and  $10 \mu\text{mol/L}$  Met-F-AEA:  $P < 0.05$ ).



were analyzed by immunoblotting for PARP cleavage at different time points (Fig. 3A). Already 6 hours after start of treatment, PARP cleavage could be observed and after 24 hours, almost no uncleaved protein was detectable. Treatment of Rh4 and Rh28 cells with increasing HU210 concentrations showed a similar increase in PARP cleavage, whereas pretreatment of Rh4 cells with  $0.5 \mu\text{mol/L}$  of the CB1-specific antagonist AM251 significantly rescued cleavage of PARP protein (Fig. 3B). At a concentration of  $1.25 \mu\text{mol/L}$  HU210, for example, the ratio of cleaved to uncleaved PARP protein could be rescued from  $1.13 (\pm 0.05 \text{ SD})$  to  $0.40 (\pm 0.03 \text{ SD})$ ; Fig. 3C).

Additionally, caspase-3 activation after 24 hours of HU210 treatment was measured in Rh4 cells (Fig. 3D). A concentration-dependent increase of cells positively stained for active caspase-3 was detected with close to 100% apoptotic cells at  $1.25 \mu\text{mol/L}$  of HU210. In line with the previous results, we also observed that both THC (2 and  $4 \mu\text{mol/L}$ ) and Met-F-AEA (5 and  $10 \mu\text{mol/L}$ ) treatment induced cleavage of PARP protein after 24 hours of incubation (Fig. 3E and F). Therefore, treatment of tposRMS with cannabinoids induces apoptosis in tposRMS cells.

#### Cannabinoids Inhibit AKT Signaling

Earlier studies investigating effects of cannabinoids on cancer cells could show alterations in AKT and ERK signaling upon drug treatment. Based on this, we next studied AKT and ERK signaling in tposRMS cells after cannabinoid treatment. Among the tposRMS cell lines, Rh4 cells most accurately reflect the translocation-specific gene expression signature and therefore this cell line was selected as model system for further studies. They were incubated with  $1.25 \mu\text{mol/L}$  HU210 for 30 minutes and 2 hours before cell

lysis. A rapid decrease in phospho-AKT at Ser<sup>473</sup> was detected, indicating inhibition of AKT activity (Fig. 4A). Under the same experimental conditions, phosphorylation of ERK was found to increase in tposRMS cells after drug treatment compared with vehicle-treated cells, at both Thr<sup>202</sup>/Tyr<sup>204</sup> (Fig. 4A, bottom left). Further phosphorylation on Thr<sup>308</sup> of AKT was also reduced. In addition, the AKT downstream target GSK3 $\beta$  became significantly dephosphorylated (Fig. 4A, right). Notably, also THC (2 and  $4 \mu\text{mol/L}$ ) as well as Met-F-AEA (5 and  $10 \mu\text{mol/L}$ ) triggered dephosphorylation of AKT at Ser<sup>473</sup> (Fig. 4B) with a slight delay compared with HU210. No difference for ERK phosphorylation was observed with either of these two substances (data not shown). In summary, all three cannabinoid agonists lead to inhibition of AKT signaling in tposRMS cells, whereas ERK activation was only seen after treatment with HU210. These experiments suggest that the AKT pathway is likely to mediate the action of cannabinoids in our tumor model.

#### Cannabinoids Reduce Viability through Up-Regulation of Transcription Factor p8

p8 is a transcription factor involved in cellular stress responses following cellular injuries through pathways implicated in growth inhibition (25, 26). Furthermore, p8 mediates apoptosis upon cannabinoid treatment of glioblastoma (19), pancreatic cancer (20), and breast cancer (21) cells. Therefore, we tested involvement of p8 in the antiproliferative action of HU210, THC, and Met-F-AEA in our model. p8 levels were assessed in mRNA isolated 16 hours after the addition of drugs to Rh4 cells. A clear dose-dependent increase in p8 transcripts up to 6.5-fold was observed for all cannabinoids used compared with vehicle-treated control samples (Fig. 5A).

To validate the requirement of p8 up-regulation for induction of apoptosis, p8 expression was specifically down-regulated by treatment with siRNA. mRNA levels after treatment were on average down to 16% ( $\pm 5.5\%$  SD) 48 hours after transfection. Upon incubation with 1.25  $\mu\text{mol/L}$  of HU210 for 48 hours, viability of scrambled-transfected cells was reduced to 37% ( $\pm 9.4$  SE), whereas cells with lower p8 transcript levels showed a rescue in viability up to 63% ( $\pm 8.5$  SE; Fig. 5B). This suggests that an increase in p8 levels after cannabinoid treatment is an important component of the molecular response. These experiments indicate that p8 mediates, at least in part,

the reduction in viability observed after cannabinoid treatment.

### HU210 Reduces Tumor Growth of tposRMS Xenografts

To test whether HU210 might have a therapeutic effect on tposRMS tumors *in vivo*, tumor xenografts were generated by s.c. injection of Rh4 cells into immunodeficient NOG mice. Tumors were treated peritumorally with HU210 daily for 13 subsequent days. We observed significantly reduced tumor growth in HU210-treated compared with vehicle-treated animals (Fig. 6). Tumors were excised after the last day of treatment and paraffin-embedded sections were

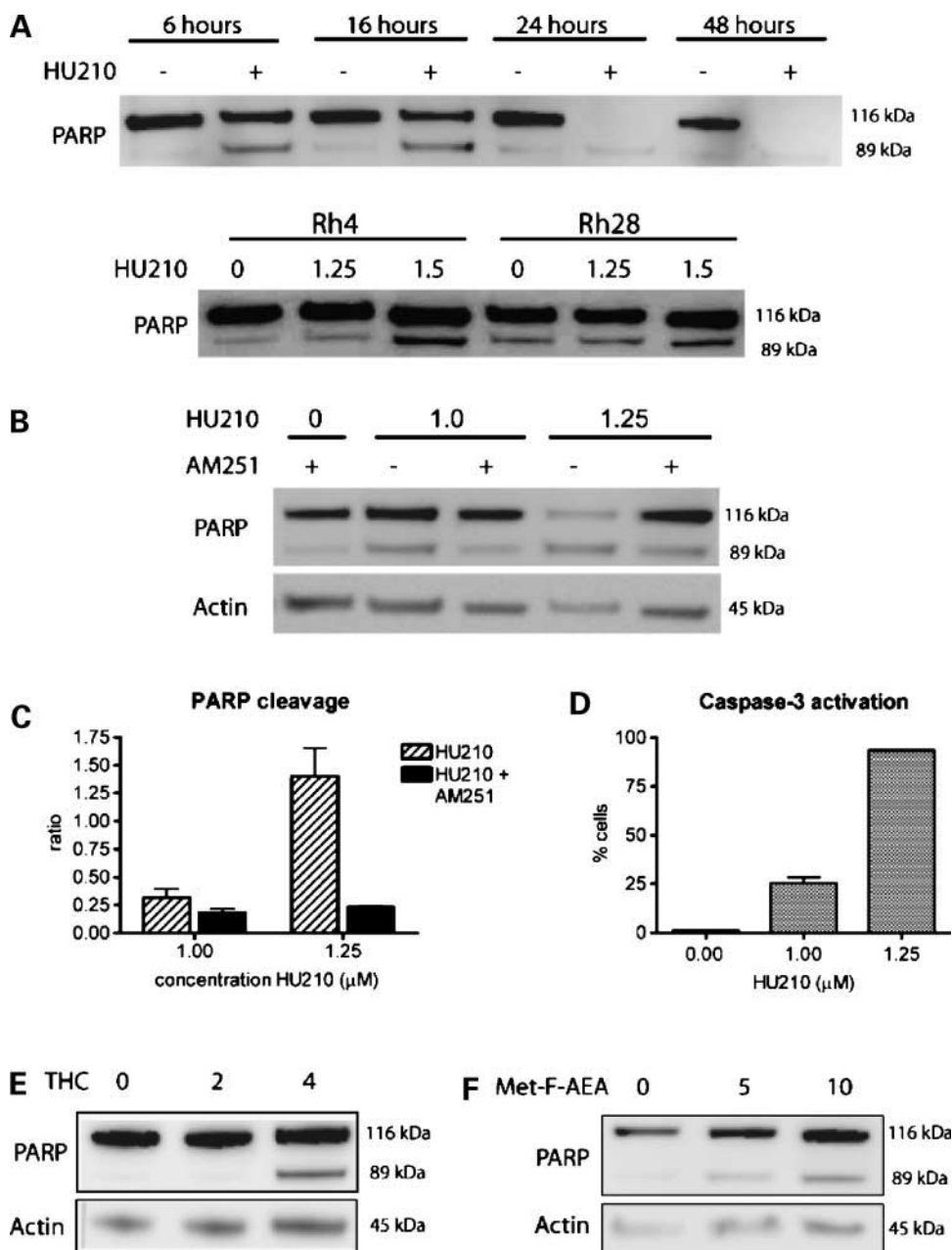
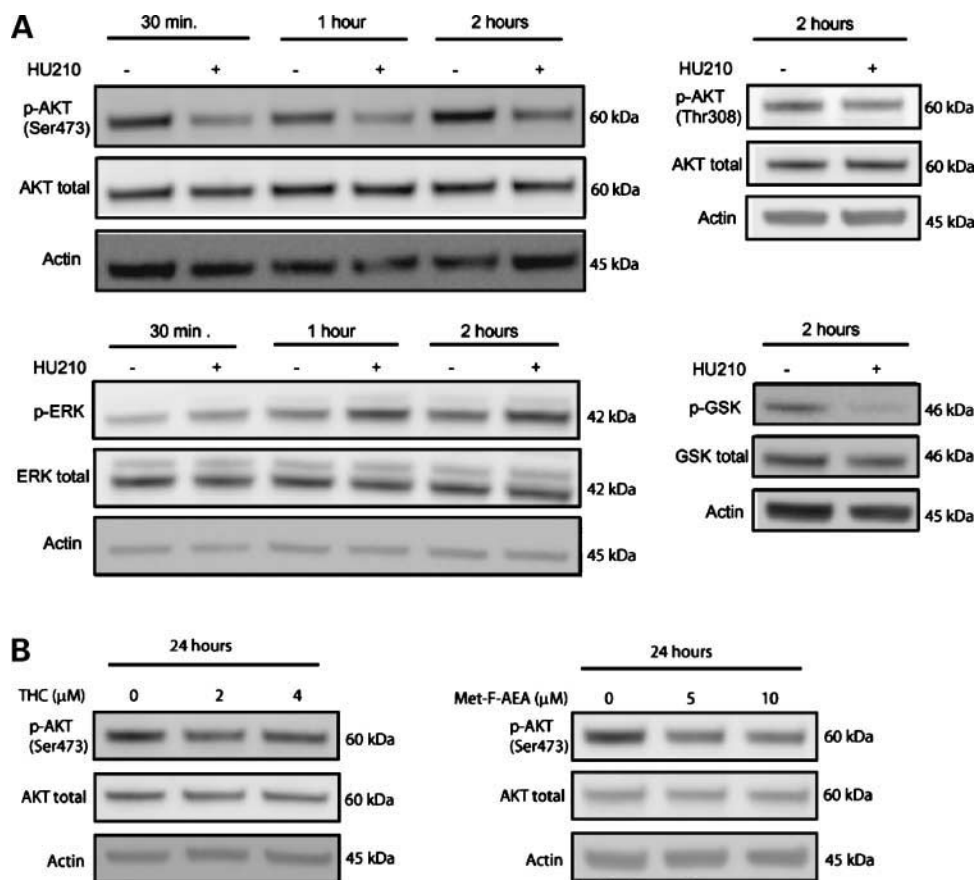


**Figure 3.** Cannabinoids induce apoptosis in tposRMS cells. **A**, Rh4 cells were treated for 6, 16, 24, and 48 h with either 1.25  $\mu\text{mol/L}$  HU210 or DMSO. Rh28 and Rh4 cell were incubated with increasing concentrations of HU210 for 24 h (*bottom*). Subsequently, Western blotting was done with an anti-PARP antibody. **B**, after preincubation of Rh4 cells with 0.5  $\mu\text{mol/L}$  of CB1 antagonist AM251, HU210 was added at concentrations of 1 and 1.25  $\mu\text{mol/L}$  HU210 for 20 h. Cell lysates were probed with anti-PARP (*top*) and anti-actin (*bottom*) by immunoblotting. **C**, densitometric quantification of the ratio of cleaved to uncleaved PARP product (values  $\pm$  SE,  $n = 2$ ). **D**, percentage of cells staining positively for proapoptotic caspase-3 is shown as evaluated after 20 h of HU210 treatment of Rh4 cells (values  $\pm$  SE,  $n = 3$ , significance  $P < 0.005$ ). Rh4 cells were either treated with 2 and 4  $\mu\text{mol/L}$  of THC (**E**) or 5 and 10  $\mu\text{mol/L}$  of Met-F-AEA (**F**) for 24 h. Protein extract was analyzed for PARP and actin by Western blotting (here shown a representative blot).

**Figure 4.** Cannabinoid receptor agonists affect AKT and ERK signaling in tposRMS cells. **A**, Rh4 cells were incubated with 1.25  $\mu\text{mol/L}$  HU210 for 30 min, 1 h, and 2 h, and cell lysates were prepared. Then, Western blotting was done with antibodies against phospho-AKT (Ser<sup>473</sup>; top left) and against phospho-ERK (bottom left). Anti-phospho-GSK (bottom right) and anti-phospho-AKT (Thr<sup>308</sup>; top right) were probed on extracts of cells treated for 2 h with 1.25  $\mu\text{mol/L}$  of HU210. **B**, phosphorylation status of AKT at Ser<sup>473</sup> was analyzed by Western blotting after treatment of Rh4 cells with 2 and 4  $\mu\text{mol/L}$  THC (top) or 5 and 10  $\mu\text{mol/L}$  Met-F-AEA (bottom) for 24 h.



either H&E stained or subsequently immunohistochemically analyzed with antibodies against the proliferation marker Ki67 and the apoptosis indicator cleaved caspase-3. H&E-stained sections from HU210-treated animals displayed a high number of cell-free patches filled with connective tissue, which are probably remains of previously apoptotic or necrotic areas. In agreement with this, a moderate increase of apoptotic cells, which was variable across tumors, was detected in HU210-treated mice compared with vehicle-treated animals (data not shown). On the other hand, no difference in the staining pattern for Ki67 was observed among treatment modalities (data not shown). In conclusion, HU210 is capable of reducing aRMS xenograft growth through induction of apoptosis *in vivo*.

## Discussion

Evidence from *in vitro* and *in vivo* experiments suggests that cannabinoid receptor agonists can reduce tumor growth and induce apoptosis in several tumor types, including melanoma, breast and prostate cancer, colon cancer, leukemia, and glioma. However, to our knowledge, the response to cannabinoid treatment has not been studied in sarcomas yet. Here, we investigated the effects of cannabinoid receptor agonists in the sarcoma tposRMS, which we not only confirmed to express high levels of CB1 mRNA but also

showed expression on the protein level by Western blot and immunohistochemistry.

*In vitro*, cannabinoid receptor agonists HU210, THC, and Met-F-AEA exerted an antiproliferative and proapoptotic action on tposRMS cells through activation of the CB1 receptor. The specificity of this effect for CB1 was shown by two means: First, the cell viability in fibroblasts or tnegRMS control cell lines, which express only low levels of CB1, is not affected. Second, the CB1-specific antagonist AM251 was able to significantly reduce apoptosis and partially restore cell viability. TposRMS cells were most sensitive to submicromolar concentrations of HU210, THC, and Met-F-AEA, and comparable with those observed in other cancer cells such as pancreatic cancer (20), breast cancer (22), or colon cancer (27) cells.

Key events contributing to cannabinoid-triggered induction of apoptosis in tposRMS cells are diminished AKT signaling and up-regulation of the transcription factor p8. Whereas cancer cells such as melanoma (11), colon cancer (17), and glioma (15) also experience dephosphorylation of AKT after cannabinoid stimulation, nontransformed CB1-expressing cells such as neurons react with increased phosphorylation of AKT under the same circumstances (16, 28). The key event responsible for this fundamental difference is still unknown; however, *de novo* ceramide synthesis (29) seems to be important for induction of apoptosis in cancer

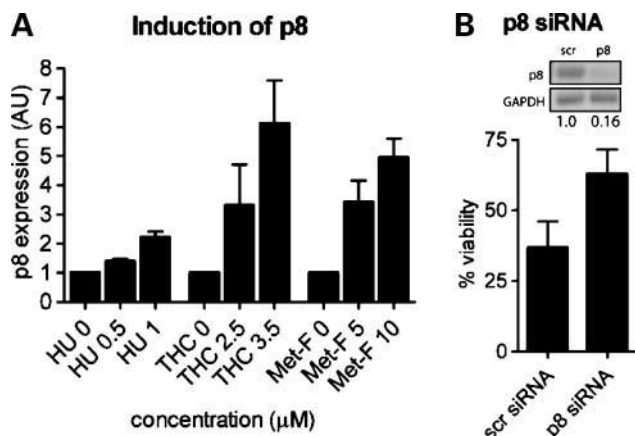


**Figure 5.** Induction of proapoptotic p8. **A**, Rh4 cells were treated with 0.5 and 1 μmol/L of HU210, 2.5 and 3.5 μmol/L of THC (**B**), or 5 and 10 μmol/L of Met-F-AEA for 16 h. RNA was extracted and analyzed for p8 transcripts with quantitative RT-PCR ( $n = 3$ ,  $\pm$ SE,  $P < 0.05$ ). Values were normalized to GAPDH. **B**, p8 was down-regulated by means of siRNA. *Top*, a representative RT-PCR and quantitative values (in arbitrary units, normalized to scrambled siRNA transfected control cells). Viability after HU210 (1.25 μmol/L) treatment was assessed at 48 h with MTT ( $n = 3$ ,  $\pm$ SE,  $P < 0.05$ ).

cells. Apart from AKT, the transcription factor p8 was recently shown to be up-regulated by cannabinoid receptor agonists and this event seems to be crucial for their sensitivity (19) because knockdown of this gene could rescue cell viability in cancer cells such as glioma (19), breast cancer (21), or pancreatic cancer (20). As shown here, also in tposRMS cells is p8 a critical mediator of proapoptotic signaling after cannabinoid treatment because inhibition of its accumulation by means of RNA interference significantly rescued cell viability. In contrast, the response of the ERK pathway is not consistent and seems to be either tumor type specific depending on the type of agonist used. Therefore, it is less likely to play an important role in our model.

Thus far, HU210 has been used in animal models to investigate neurogenesis (30) and multiple sclerosis (31) and was recently shown to prevent formation of preneoplastic lesions in mouse colon (32). However, HU210 treatment of xenograft-bearing mice has not been reported thus far. Here, we observed significantly reduced tumor growth in HU210-treated animals without overt psychoactive signs. Growth reduction observed was comparable with other xenograft models treated with cannabinoids, such as treatment of pancreatic cancer tumors with THC or JWH-133 (20). A moderate increase in the number of apoptotic cells was observed in HU210-treated xenograft sections; however, we cannot exclude other mechanisms to additionally account for reduction in tumor growth. However, analysis of transcript levels of myogenic differentiation markers, such as myosin light chain or troponin C (33), did not significantly differ between treatment modalities, ruling out the possibility that cannabinoids induce differentiation in tposRMS cells as observed after inhibition of PAX3/FKHR function.

In comparison with other drug classes such as the broad-spectrum kinase inhibitor PKC412 investigated in our laboratory (34), HU210 treatment as single agent seems less efficient in tumor growth reduction. Nevertheless, potential use of cannabinoids as therapeutic intervention for tposRMS should still be pursued, possibly in combination with conventional chemotherapies, kinase inhibitors, or other targeted agents. Several reports indicate synergistic activity of cannabinoid receptor agonists in combination with well-established antineoplastic substances. THC was reported to act synergistically with suboptimal doses of doxorubicin or cisplatin (19), and synergism between HU210 and 5-fluorouracil was recently reported as well (27).

In summary, our results support and extend the previously shown antitumor activities of cannabinoid receptor agonists by showing proapoptotic effects of HU210, THC, and Met-F-AEA on tposRMS cells *in vitro* and, for

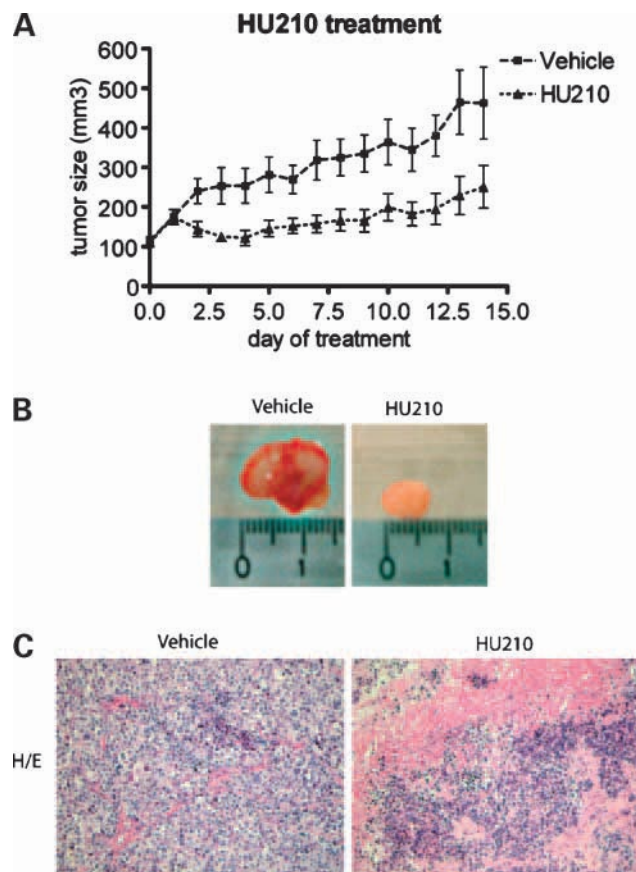


**Figure 6.** HU210 reduces tumor growth *in vivo*. NOG mice were injected with  $7.5 \times 10^6$  tposRMS (Rh4) cells s.c. into the flank. After reaching a tumor size of 100 to 150 mm<sup>3</sup>, animals were assigned randomly to either the vehicle ( $n = 7$ ) or the HU210 ( $n = 6$ ) group. Treatment was given daily by injecting either 0.2 mg/kg HU210 or DMSO in PBS peritumorally for 13 d, whereas tumor growth was monitored daily and mice were sacrificed on the day after the last treatment. **A**, tumor growth over time is shown for HU210-treated compared with vehicle-treated animals ( $\pm$ SE,  $P < 0.001$ ). **B** and **C**, representative sections of tumors from vehicle- and HU210-treated animals were stained with H&E. Original magnification, 100 $\times$ .

the first time, show that HU210 has tumor growth inhibiting properties *in vivo*. This could represent one possible novel treatment strategy that might improve outcome in this pediatric tumor.

## Disclosure of Potential Conflicts of Interest

No potential conflicts of interests were disclosed.

## Acknowledgments

We thank Cristina Blazquez and Tania Aguado for their support and Beat Bornhauser for breeding of the NOG mice.

## References

- Pappo AS. Rhabdomyosarcoma and other soft tissue sarcomas of childhood. *Curr Opin Oncol* 1995;7:361–6.
- Koscielniak E, Harms D, Henze G, et al. Results of treatment for soft tissue sarcoma in childhood and adolescence: a final report of the German Cooperative Soft Tissue Sarcoma Study CWS-86. *J Clin Oncol* 1999;17:3706–19.
- Shapiro DN, Sublett JE, Li B, Downing JR, Naevae CW. Fusion of PAX3 to a member of the forkhead family of transcription factors in human alveolar rhabdomyosarcoma. *Cancer Res* 1993;53:5108–12.
- Wachtel M, Dettling M, Koscielniak E, et al. Gene expression signatures identify rhabdomyosarcoma subtypes and detect a novel t(2;2)(q35;p23) translocation fusing PAX3 to NCOA1. *Cancer Res* 2004;64:5539–45.
- Davicioni E, Finckenstein FG, Shahbazian V, Buckley JD, Triche TJ, Anderson MJ. Identification of a PAX-FKHR gene expression signature that defines molecular classes and determines the prognosis of alveolar rhabdomyosarcomas. *Cancer Res* 2006;66:6936–46.
- Lae M, Ahn EH, Mercado GE, et al. Global gene expression profiling of PAX-FKHR fusion-positive alveolar and PAX-FKHR fusion-negative embryonal rhabdomyosarcomas. *J Pathol* 2007;212:143–51.
- Taulli R, Scuoppo C, Bersani F, et al. Validation of met as a therapeutic target in alveolar and embryonal rhabdomyosarcoma. *Cancer Res* 2006;66:4742–9.
- Munson AE, Harris LS, Friedman MA, Dewey WL, Carchman RA. Anti-neoplastic activity of cannabinoids. *J Natl Cancer Inst* 1975;55:597–602.
- Sanchez C, Galve-Roperh I, Canova C, Brachet P, Guzman M.  $\Delta^9$ -Tetrahydrocannabinol induces apoptosis in C6 glioma cells. *FEBS Lett* 1998;436:6–10.
- De Petrocellis L, Melck D, Palmisano A, et al. The endogenous cannabinoid anandamide inhibits human breast cancer cell proliferation. *Proc Natl Acad Sci U S A* 1998;95:8375–80.
- Blazquez C, Carracedo A, Barrado L, et al. Cannabinoid receptors as novel targets for the treatment of melanoma. *FASEB J* 2006;20:2633–5.
- Guzman M. Cannabinoids: potential anticancer agents. *Nat Rev Cancer* 2003;3:745–55.
- Galve-Roperh I, Sanchez C, Cortes ML, del Pulgar TG, Izquierdo M, Guzman M. Anti-tumoral action of cannabinoids: involvement of sustained ceramide accumulation and extracellular signal-regulated kinase activation. *Nat Med* 2000;6:313–9.
- Guzman M, Duarte MJ, Blazquez C, et al. A pilot clinical study of  $\Delta^9$ -tetrahydrocannabinol in patients with recurrent glioblastoma multiforme. *Br J Cancer* 2006;95:197–203.
- Gomez del Pulgar T, Velasco G, Sanchez C, Haro A, Guzman M. *De novo*-synthesized ceramide is involved in cannabinoid-induced apoptosis. *Biochem J* 2002;363:183–8.
- Gomez del Pulgar T, Velasco G, Guzman M. The CB1 cannabinoid receptor is coupled to the activation of protein kinase B/Akt. *Biochem J* 2000;347:369–73.
- Greenhough A, Patsos HA, Williams AC, Paraskeva C. The cannabinoid  $\delta(9)$ -tetrahydrocannabinol inhibits RAS-MAPK and PI3K-AKT survival signalling and induces BAD-mediated apoptosis in colorectal cancer cells. *Int J Cancer* 2007;121:2172–80.
- Melck D, Rueda D, Galve-Roperh I, De Petrocellis L, Guzman M, Di Marzo V. Involvement of the cAMP/protein kinase A pathway and of mitogen-activated protein kinase in the anti-proliferative effects of anandamide in human breast cancer cells. *FEBS Lett* 1999;463:235–40.
- Carracedo A, Lorente M, Egia A, et al. The stress-regulated protein p8 mediates cannabinoid-induced apoptosis of tumor cells. *Cancer Cell* 2006;9:301–12.
- Carracedo A, Gironella M, Lorente M, et al. Cannabinoids induce apoptosis of pancreatic tumor cells via endoplasmic reticulum stress-related genes. *Cancer Res* 2006;66:6748–55.
- Caffarel MM, Moreno-Bueno G, Cerutti C, et al. JunD is involved in the antiproliferative effect of  $\Delta^9$ -tetrahydrocannabinol on human breast cancer cells. *Oncogene* 2008;27:5033–44.
- Caffarel MM, Sarrio D, Palacios J, Guzman M, Sanchez C.  $\Delta^9$ -Tetrahydrocannabinol inhibits cell cycle progression in human breast cancer cells through Cdc2 regulation. *Cancer Res* 2006;66:6615–21.
- Galanti G, Fisher T, Kventzel I, et al.  $\Delta^9$ -Tetrahydrocannabinol inhibits cell cycle progression by downregulation of E2F1 in human glioblastoma multiforme cells. *Acta Oncol* 2007;1–9.
- Ellert-Miklaszewska A, Kaminska B, Konarska L. Cannabinoids down-regulate PI3K/Akt and Erk signalling pathways and activate proapoptotic function of Bad protein. *Cell Signal* 2005;17:25–37.
- Encinar JA, Mallo GV, Mizyrycki C, et al. Human p8 is a HMG-I/Y-like protein with DNA binding activity enhanced by phosphorylation. *J Biol Chem* 2001;276:2742–51.
- Malicet C, Lesavre N, Vasseur S, Iovanna JL. p8 inhibits the growth of human pancreatic cancer cells and its expression is induced through pathways involved in growth inhibition and repressed by factors promoting cell growth. *Mol Cancer* 2003;2:37.
- Gustafsson SB, Lindgren T, Jonsson M, Jacobsson SO. Cannabinoid receptor-independent cytotoxic effects of cannabinoids in human colorectal carcinoma cells: synergism with 5-fluorouracil. *Cancer Chemother Pharmacol* 2008.
- Ozaita A, Puighermanal E, Maldonado R. Regulation of PI3K/Akt/GSK-3 pathway by cannabinoids in the brain. *J Neurochem* 2007;102:1105–14.
- Velasco G, Galve-Roperh I, Sanchez C, Blazquez C, Haro A, Guzman M. Cannabinoids and ceramide: two lipids acting hand-by-hand. *Life Sci* 2005;77:1723–31.
- Jiang W, Zhang Y, Xiao L, et al. Cannabinoids promote embryonic and adult hippocampus neurogenesis and produce anxiolytic- and antidepressant-like effects. *J Clin Invest* 2005;115:3104–16.
- Docagne F, Muneton V, Clemente D, et al. Excitotoxicity in a chronic model of multiple sclerosis: neuroprotective effects of cannabinoids through CB1 and CB2 receptor activation. *Mol Cell Neurosci* 2007;34:551–61.
- Izzo AA, Aviello G, Petrosino S, et al. Increased endocannabinoid levels reduce the development of precancerous lesions in the mouse colon. *J Mol Med* 2008;86:89–98.
- Ebauer M, Wachtel M, Niggli FK, Schafer BW. Comparative expression profiling identifies an *in vivo* target gene signature with TFAP2B as a mediator of the survival function of PAX3/FKHR. *Oncogene* 2007;26:7267–81.
- Amstutz R, Wachtel M, Troxler H, et al. Phosphorylation regulates transcriptional activity of PAX3/FKHR and reveals novel therapeutic possibilities. *Cancer Res* 2008;68:3767–76.



# Molecular Cancer Therapeutics

## Cannabinoid receptor 1 is a potential drug target for treatment of translocation-positive rhabdomyosarcoma

Susanne Oesch, Dagmar Walter, Marco Wachtel, et al.

*Mol Cancer Ther* 2009;8:1838-1845. Published OnlineFirst June 9, 2009.

**Updated version** Access the most recent version of this article at:  
doi:[10.1158/1535-7163.MCT-08-1147](https://doi.org/10.1158/1535-7163.MCT-08-1147)

**Cited articles** This article cites 32 articles, 10 of which you can access for free at:  
<http://mct.aacrjournals.org/content/8/7/1838.full#ref-list-1>

**Citing articles** This article has been cited by 2 HighWire-hosted articles. Access the articles at:  
<http://mct.aacrjournals.org/content/8/7/1838.full#related-urls>

**E-mail alerts** [Sign up to receive free email-alerts](#) related to this article or journal.

**Reprints and Subscriptions** To order reprints of this article or to subscribe to the journal, contact the AACR Publications Department at [pubs@aacr.org](mailto:pubs@aacr.org).

**Permissions** To request permission to re-use all or part of this article, use this link  
<http://mct.aacrjournals.org/content/8/7/1838>.  
Click on "Request Permissions" which will take you to the Copyright Clearance Center's (CCC) Rightslink site.